Mechanical Properties of Gels Formed by Nickel and Cobalt Complexation with Histamine-Grafted Polyisoprene and Polystyrene in Non-Aqueous Solvents

by

Omar A. Laris

Submitted to the
Department of Materials Science and Engineering
in Partial Fulfillment of the Requirements for the Degree of

Bachelor of Science

at the

Massachusetts Institute of Technology

June 2020

Signature of Author……
Department of Materials Science and Engineering
May 1, 2020

Certified By……
Niels Holten-Andersen
Associate Professor of Materials Science and Engineering
Thesis Supervisor

Accepted By……...
Juejun Hu
Associate Professor of Materials Science and Engineering
Chair, DMSE Undergraduate Committee

Mechanical Properties of Gels Formed by Nickel and Cobalt Complexation with Histamine-Grafted Polyisoprene and Polystyrene in Non-Aqueous Solvents

by

Omar A. Laris

Submitted to the Department of Materials Science and Engineering
on May 1, 2020
in Partial Fulfillment of the Requirements for the Degree of
Bachelor of Science at the Massachusetts Institute of Technology

Abstract

Leveraging metal-coordination crosslinks for materials design of polymers can enable fine-tuning of the mechanical properties of rubbers without requiring the use of sophisticated vulcanization pathways. In this work, we synthesized several polyisoprene-graft-histamine gels in toluene, coordinated by Ni^{2+} and Co^{2+} ions. In addition, we synthesized polystyrene-graft-histamine-$Ni(OH)_2$ composites in DMF, with $Ni(OH)_2$ nanoparticles nucleated and grown *in situ* upon the addition of a hydroxide. The viscoelastic mechanical properties of these materials are improved relative to the base polymers.

Thesis Supervisor: Niels Holten-Andersen
Title: Associate Professor of Materials Science and Engineering

Acknowledgements

I am deeply grateful to Professor Holten-Andersen for his mentorship throughout this thesis project. Even while weathering a world in crisis, he provided support and feedback every step of the way. I would also like to thank Jake Song for continually pushing me to deepen my understanding of the fundamental science involved in this project, and for helping me become a much more effective researcher by putting knowledge into practice.

Table of Contents

List of Figures

1. Introduction

1.1 Motivation

Metal coordination bonding in polymers is a burgeoning field of research due to its potential as a materials design platform to tune the mechanical properties of soft matter. Metal coordination bonding provides an alternative to conventional covalent crosslinking (vulcanization) in rubbers, which form irreversible bonds[1]. Previous research into metal coordination bonding in polymer systems has primarily been performed in aqueous environments, which is applicable to soft matter applications in the biomedical field but precludes many commercial applications where dissolution in water is undesirable[2]. Additionally, much of the work has been focused on the synthesis of supramolecular networks of small or oligomeric molecules held together by metal-coordination bonds[3]. Self-assembly of hydrogels in the presence of nanoparticles due to metal coordination bonding has also been established previously[4]. In this work, we aim to explore the relationship between the design parameters of metal ion identity and nanoparticle presence, and the resultant mechanical properties of non-aqueous polymer networks which can participate in metal-coordination bonding.

The development of a design framework for such materials builds on previous work in hydrogel systems which demonstrate the gelling effect of metal ions when in the presence of the coordinating ligands[3]. Additionally, nanoparticle-gel composites have been fabricated previously, both by mixing and by *in-situ* mineralization[4]. Inspiration for the design of these materials has been drawn from the organic-inorganic composites found in natural materials such as nacre and chiton. Understanding the interplay between the organic and inorganic components

of these materials can enable the design of new materials with self-healing properties and precise control of mechanical properties in and out of water.

1.2 Applications

The applications of this materials design framework extend to the commercial materials sector currently occupied by vulcanized rubbers as well as the biomedical device industry. The vulcanization of rubbers today is performed via complex chemical reactions at elevated temperatures[1]. Metal-coordination crosslinking can present an alternative to this processing by yielding a solution-based processing method in which elevated temperatures become obsolete, and whereby the appropriate choice of ligands and metal ions would allow the crosslink bonding strength to approach that of many conventional covalent bonds[5,6]. Additionally, the reversibility of metal-coordination crosslinking enables solution-based recycling pathways which can, through alterations to pH or voltage, control crosslinking[4]. Improvements in rubber recycling could limit waste generated from vulcanized rubbers, waste which currently cannot easily be devulcanized or returned to an un-crosslinked state.

2. Background

2.1 Reversible metal-coordination bonding in hydrogel systems

Coordination bonding between metal ions and organic complexes such as azoles, azines, and ethers is at the root of the material structure and organization of networks of organometallic molecules[5]. Hydrogels can be formed from the coordination of metal ions by macromolecules such as catechol-bearing polymers by enabling cross-linking between the catechols[7]. Common choices for the backbone polymer are multi-arm polymers which enable high degrees of network connectivity. Various complexes may be formed between the metal ions and the ligands depending on the valency of the metal ion, a parameter which can be electrochemically modulated[8]. The reversibility of metal-coordination bonding in the resulting hydrogels enables self-healing properties upon tensile failure or non-linear mechanical disturbance of the polymer network. Furthermore, the linear mechanical properties of these hydrogels are functions of various parameters, including but not limited to: ion identity, coordination character between the ion and coordinating ligands, the identity of the ligand-bearing molecule, choice of solvent, and ion concentration.

The gelation of organic molecules via metal coordination bonding presents an opportunity for the design of bio-compatible soft matter for use in biomedical devices as well as stimuli-responsive materials as is necessary for the next iteration of soft robotics. The vast parameter space of this materials class presents a challenge for research, which occurs at the intersection of metal-organic chemistry, mechanics, and materials science.

2.2 In-situ mineralization in hydrogels & biological materials

Biomineralization is a phenomenon widespread in nature whereby organisms construct mineralized material structures[9]. Biomineralized structures are frequently ordered over many length scales, and do not follow conventional models of crystallization. Exhibiting finely controlled microstructures composed of both precipitated minerals and organic molecules, biomineralized materials oftentimes present desirable mechanical properties, but their formation is not well-understood[10]. Research suggests that ligating proteins play roles in the mediation of mineral nucleation and growth[11]. Nanoparticle-hydrogel composites are emerging as promising candidates for a suite of applications, including electrodes, anti-microbial coatings, stimuli-responsive materials, and fluorescent bio-markers[12]

In-situ mineralization in hydrogels employs a biomimetic approach to materials design by utilizing metal-coordination hydrogels as a matrix within which minerals are precipitated. The advantage of *in-situ* nanoparticle growth is the ability to control the nanoparticle size by controlled addition of oxidizers and additional metal ions. Various nanoparticles have been explored for the production of nanocomposite hydrogels, including transition metal oxides, alkali oxides, and non-metallic nanoparticles[12]. In order to realize the potential of nanocomposite hydrogels as smart and multifunctional materials, tailored mechanical properties will be important.

3. Materials and Methods

3.1 Methodology

The general strategy adhered to in this investigation is as follows. First, ligand pendant groups are grafted onto a functionalizable copolymer. Next, both polymer and metal salts are solvated in non-aqueous media and mixed. UV-Vis spectroscopy testing is performed to verify coordination bonding is occurring by comparing the UV-Vis spectra with a solution of metal salts and free ligands in the same solvent. Rheological testing is performed on samples with metal ions, comparing the results with samples without ions to determine the mechanical effects of coordination. The samples are tested while still swollen with solvent to prevent entanglement from dominating the mechanical response, as the density of grafted ligands is low. For nanoparticle composites, the strategy is modified by the addition of a metal hydroxide after gelation to induce the growth of metal oxide nanoparticles within the gel. A detailed description of material choices and synthesis is presented hereafter.

3.2 Material Selection

3.2.1 Poly-Isoprene

Polyisoprene (PI) is a water-insoluble polymer with a carbon backbone and a CH_3 pendant group as depicted in Figure 1. The polymer is ubiquitous in commercial applications and has demonstrated co-polymerization pathways which make it an ideal candidate for functionalization via co-polymerization.

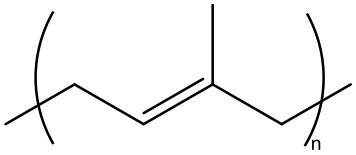

Figure 1: Molecular Structure Polyisoprene

3.2.2 Poly-Styrene

Polystyrene (PS) is a water-insoluble polymer with a carbon backbone and a C_6 aromatic ring pendant group as illustrated in Figure 2. Polystyrene is found widely in food packaging and can be co-polymerized to form graft copolymers.

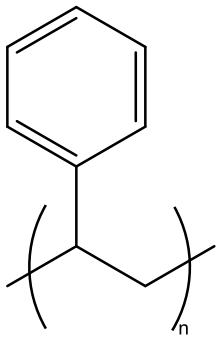

Figure 2: Molecular Structure Polystyrene

3.2.3 Maleic Anhydride

Maleic Anhydride (MA) is a reactive molecule which can be grafted into polymer chains to enable polymer functionalization. The structure is presented in Figure 3. Copolymerization with maleic anhydride bearing monomers yields a polymer which can be further modified with new pendant groups.

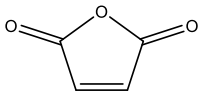

Figure 3: Molecular Structure Maleic Anhydride

3.2.4 Imidazole

Imidazole is an aromatic nitrogenous organic compound $C_3H_4N_2$ with a ring structure as illustrated in Figure 4. Imidazole participates in metal coordination bonding and is a common ligand in metal-coordination bonding research.

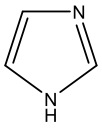

Figure 4: Molecular Structure Imidazole

3.2.5 Histamine

Histamine is a nitrogenous compound $C_5H_9N_3$, bearing an imidazole ring which can participate in metal coordination bonding. Due to the imidazole ring, comparison with imidazole is straightforward. The structure is presented in Figure 6.

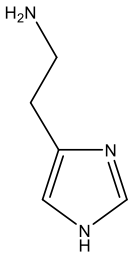

Figure 5: Molecular Structure Histamine

3.1.6 Metal Salts

Nickel and cobalt metal salts dissociate in solution, freeing Ni and Co ions to interact with metal-coordination sites on the polymers. The ions have different bond energies when interacting with the same ligand[5]. Additionally, nickel and cobalt have differing coordination numbers of 4 and 6, respectively. Various metal salts were compared in this research, listed below.

Nickel Chloride is a metal salt with the formula NiCl2. It is soluble in polar solvents.

Nickel stearate is a metal salt of nickel and stearate with formula $Ni(H_3C(CH_2)_{16}CO_2)_2$. It is soluble in toluene.

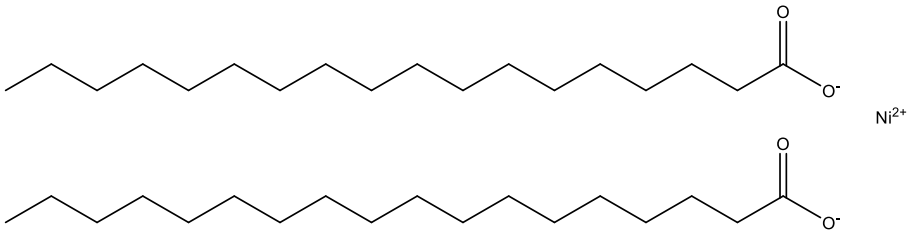

Figure 6: Molecular Structure, Nickel Stearate

Nickel and cobalt acetylacetonates are metal salts with the general formula $M(C_5H_7O_2)_2$. Acetylacetonates are common precursors for nanoparticle growth in solutions, undergoing thermal decomposition and then oxidation[13]. They are typically soluble in polar and nonpolar solvents.

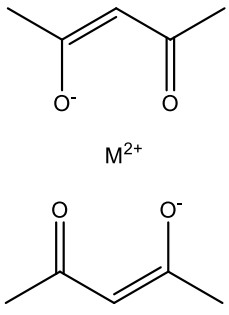

Figure 7: Molecular Structure, M(II) Acetylacetonate

3.2 Synthesis Procedures

3.2.1 Synthesis of PIMA-ion organogels

Polyisoprene-graft-maleic anhydride (PIMA) was obtained from Sigma Aldrich with M_w~25,000 and a graft density of ~1.5 wt% maleic anhydride. The maleic anhydride monomers were functionalized with histamine at various histamine to maleic anhydride ratios using the reaction pathway illustrated in Step 1 of Figure 8, performed in chloroform. This synthesis was performed by collaborators at Lincoln Laboratory and the samples listed in Table 1 were provided for experimentation.

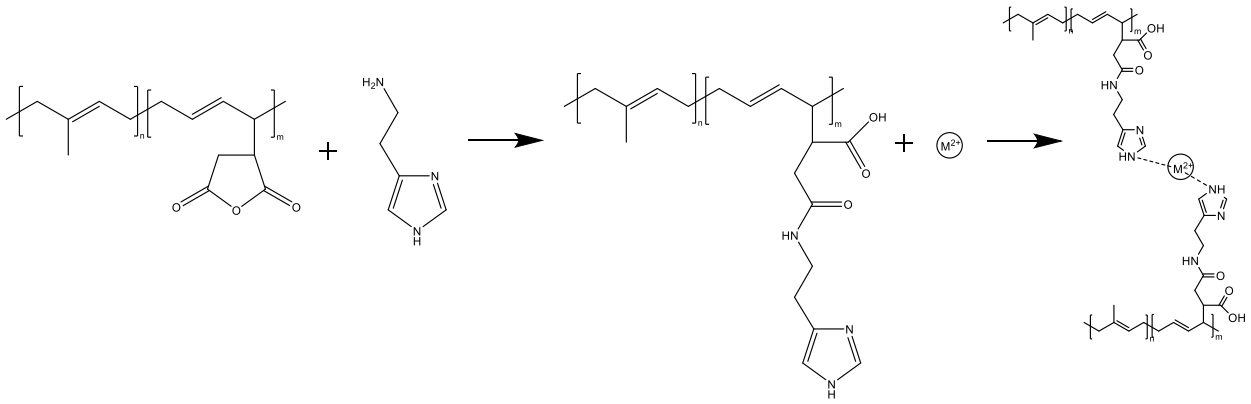

Figure 8: Synthesis of PIMA Organogels, Illustrated

Table 1. PIMA Samples, as provided

Sample ID	Backbone Functionality	Mass Ratio of Histamine/Maleic Anhydride
PIMA-1	Poly(isoprene)	0.1
PIMA-2	Poly(isoprene)	0.08
PIMA-3	Poly(isoprene)	0.06
PIMA-4	Poly(isoprene)	0.04
PIMA-5	Poly(isoprene)	0.02
PIMA-C	Poly(isoprene)	0

Chloroform was driven off to produce a solid product. PIMA was then solubilized in toluene to produce a solution of 10wt% PIMA by agitation on a vortex mixer for 10 minutes, followed by leaving at room temperature overnight to fully dissolve. The PIMA solution was

gelled by the addition metal salts solvated in toluene. The metal salt solution was prepared by dissolution in toluene at 90 ºC. The solution was pipetted into the vial of PIMA solution while still at elevated temperature, at which point the vial was agitated on a vortex mixer until homogenized. A table of samples is presented in Table 2. The ion to imidazole ratios were chosen based on the coordination number of bonding, which is 1:4 for nickel and 1:6 for cobalt. Pictures of selected samples are presented in Figure 9:.

Table 2: Synthesized PIMA gels

Metal Salt	wt% in Toluene	Ion : Imidazole Ratio
Nickel Stearate	1	1:1
Nickel Stearate	1	1:4
Nickel Acetylacetonate	1	1:1
Nickel Acetylacetonate	1	1:4
Cobalt Acetylacetonate	2.5	1:1
Cobalt Acetylacetonate	2.5	1:6

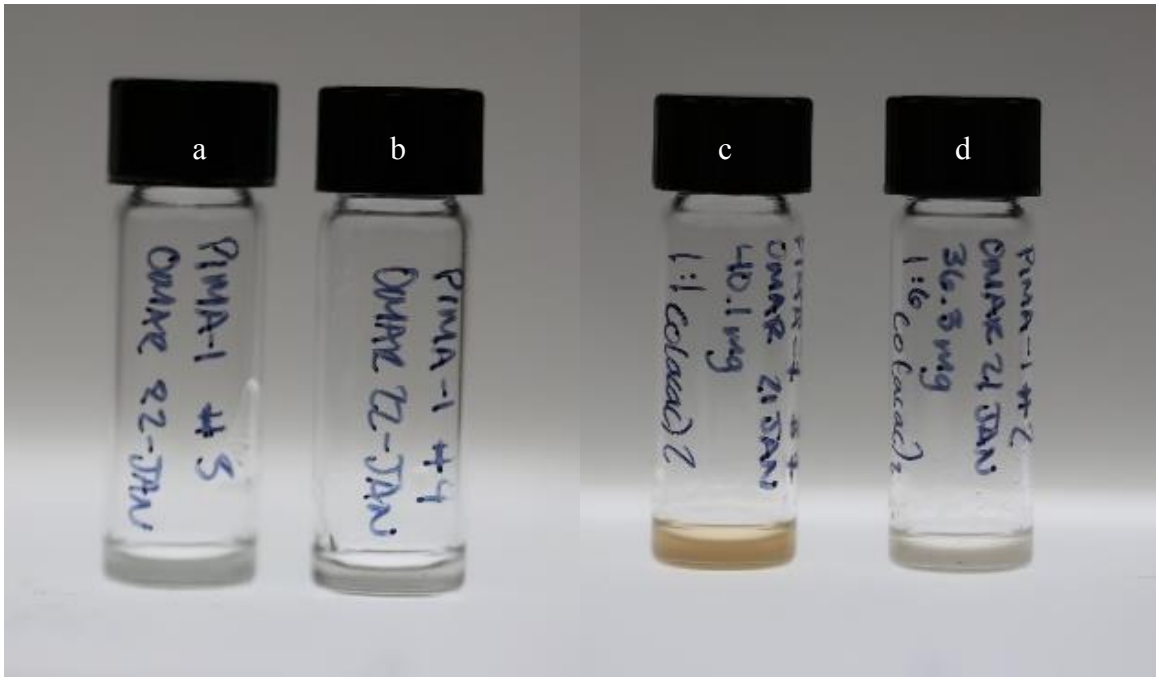

Figure 9: Optical Photographs of PIMA Samples

a) PIMA-1 with $Ni(acac)_2$ 1:1 b) PIMA-1 with $Ni(acac)_2$ 1:4
c) PIMA-1 with $Co(acac)_2$. This was the only sample with a color change visible to the naked eye. d) PIMA-1 with $Co(acac)_2$ 1:6

3.2.2 Synthesis of PSMA-NP gels

Polystyrene-graft-maleic anhydride (PSMA) was obtained from Sigma Aldrich with $M_n \sim$ 1900 and a graft density of ~25 wt% maleic anhydride. The maleic anhydride monomers were functionalized with histamine at various histamine to maleic anhydride ratios via Step 1 of the reaction pathway illustrated in Figure 10, performed in chloroform. This synthesis was carried out by collaborators at Lincoln Laboratory and the samples listed in Table 3 were provided for experimentation.

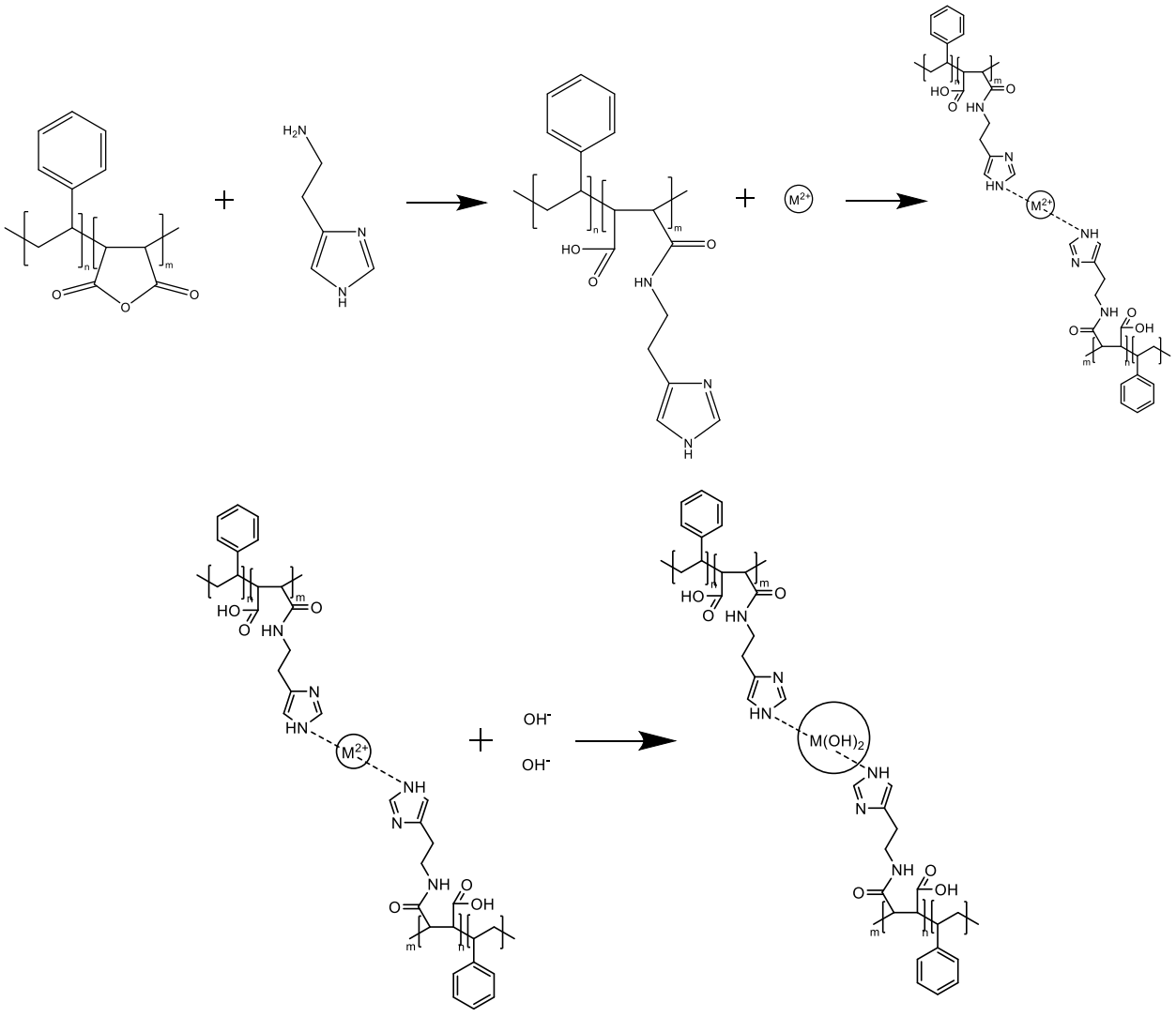

Figure 10: Synthesis of PSMA NP Organogels, Illustrated

Table 3: PSMA Samples

Sample ID	Backbone Functionality	Ratio of Histamine/Maleic Anhydride *
PSMA-1	Poly(styrene)	1
PSMA-2	Poly(styrene)	0.5
PSMA-3	Poly(styrene)	0.1
PSMA-C	Poly(styrene)	0

The chloroform was evaporated to produce a solid product. Prior to gel formation, the solubility limit of PSMA in DMF was found to be close to 30 wt% by iterated addition of DMF to a fixed amount of PSMA. After each addition of DMF, the mixture was agitated on a vortex mixer. Following the determination of the solubility limit, PSMA was added to a 0.1M NiCl2 solution using the stoichiometric ratios presented in Table 4. The mixture was agitated on a vortex mixer until fully dissolved.

After the PSMA was mixed with the NiCl2, a 1M solution of aqueous NaOH was added in a 2:1 ratio of hydroxide to nickel ions in order to precipitate metal oxide nanoparticles of $Ni(OH)_2$. The various samples synthesized are presented in Table 4, and an optical photograph of selected samples is presented in Table 4.

Table 4: Synthesized PSMA Gels

Sample	Ni : Histamine Ratio	OH : Ni Ratio
PSMA-2 + DMF	-	-
PSMA-2 + NiCl2	1:4	-
PSMA-2 + NiCl2 + NaOH	1:4	2:1
NiCl2 + NaOH	-	2:1

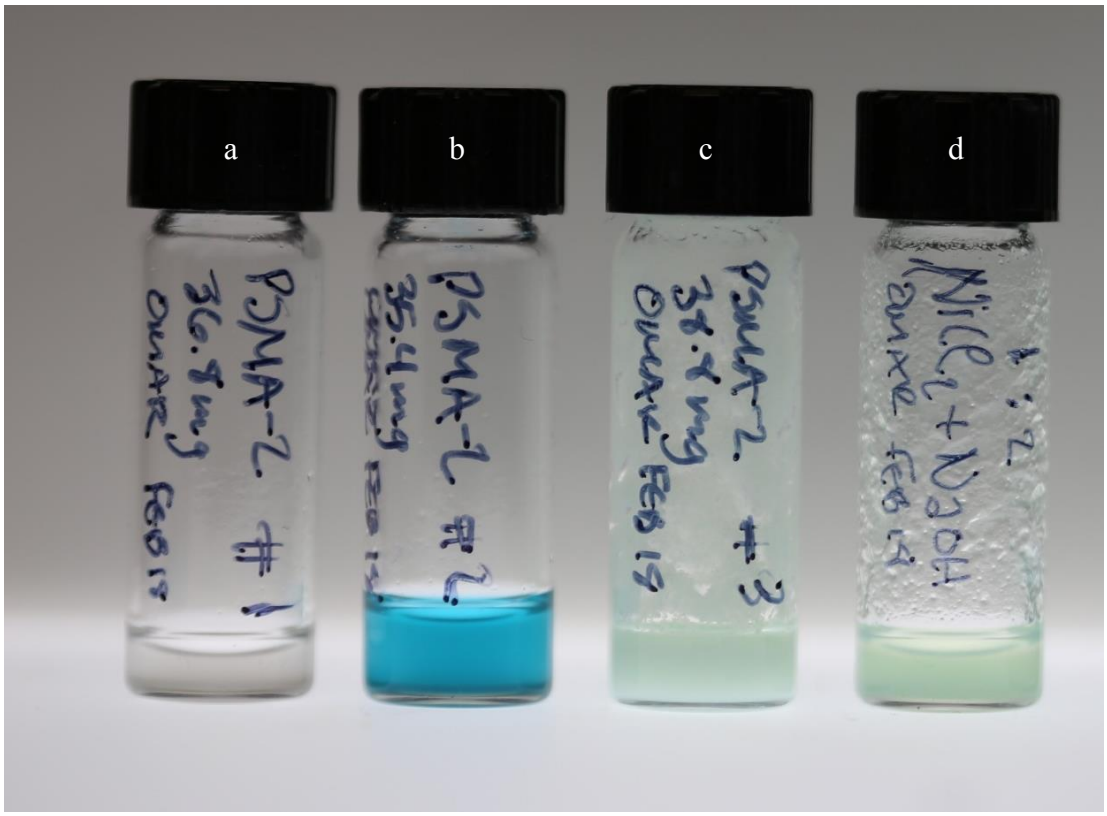

Figure 11: Optical Photographs of PSMA Samples
a) PSMA-2 in DMF 30 wt% b) PSMA-2 with NiCl2 in DMF c) PSMA-2 with NiCl2 and NaOH. The cloudiness is indicative of a precipitation product in the sample. d) NiCl2 and NaOH. The cloudiness indicates the presence of a precipitation product.

4. Characterization

4.1 UV-Vis Spectroscopy

UV-Vis Spectroscopy was used to determine whether metal coordination bonding was occurring in the organogels after the addition of metal ions. A microvolume of solution was pipetted at room temperature and placed on the testing stage. UV-Vis spectra in the wavelength range 300nm – 750 nm were collected from the following samples listed in Table 5.

Table 5: UV-Vis Samples

Sample
PIMA-1, 10 wt % in Toluene
PIMA-1 + Nickel Stearate, 1:1 Imidazole Ion Ratio
PIMA-1 + Nickel Acetylacetonate, 1:1 Imidazole Ion Ratio
PIMA-1 + Cobalt Acetylacetonate, 1:1 Imidazole Ion Ratio
Imidazole, 2.5 wt % in Toluene
Imidazole + Nickel Stearate, 1:1 Imidazole Ion Ratio
Imidazole + Nickel Acetylacetonate, 1:1 Imidazole Ion Ratio
Imidazole + Cobalt Acetylacetonate, 1:1 Imidazole Ion Ratio
Nickel Stearate, 2.5 wt % in Toluene
Nickel Acetylacetonate, 1 wt % in Toluene
Cobalt Acetylacetonate, 2.5 wt % in Toluene

4.2 Rheology

Rheological testing was used to determine the impact of ion concentration and nanoparticle growth on the mechanical response of the synthesized materials. Approximately 80 microliters of material were placed on the rheometer stage. Dynamic measurements varied shear rate from 0.1 to 100 rad/s to collect the elastic storage modulus and the viscous loss modulus. To prevent evaporation, a solvent trap filled with water was used. Samples tested are listed in Table 6.

Table 6: Rheology Samples

Sample
PIMA-1
PIMA-1 + Nickel Stearate
PIMA-1 + Cobalt Acetylacetonate
PSMA-2
Nickel Chloride + NaOH
PSMA-2 + Nickel Chloride
PSMA-2 + Nickel Chloride + NaOH

5. Results and Discussion

5.1 UV-Vis Results

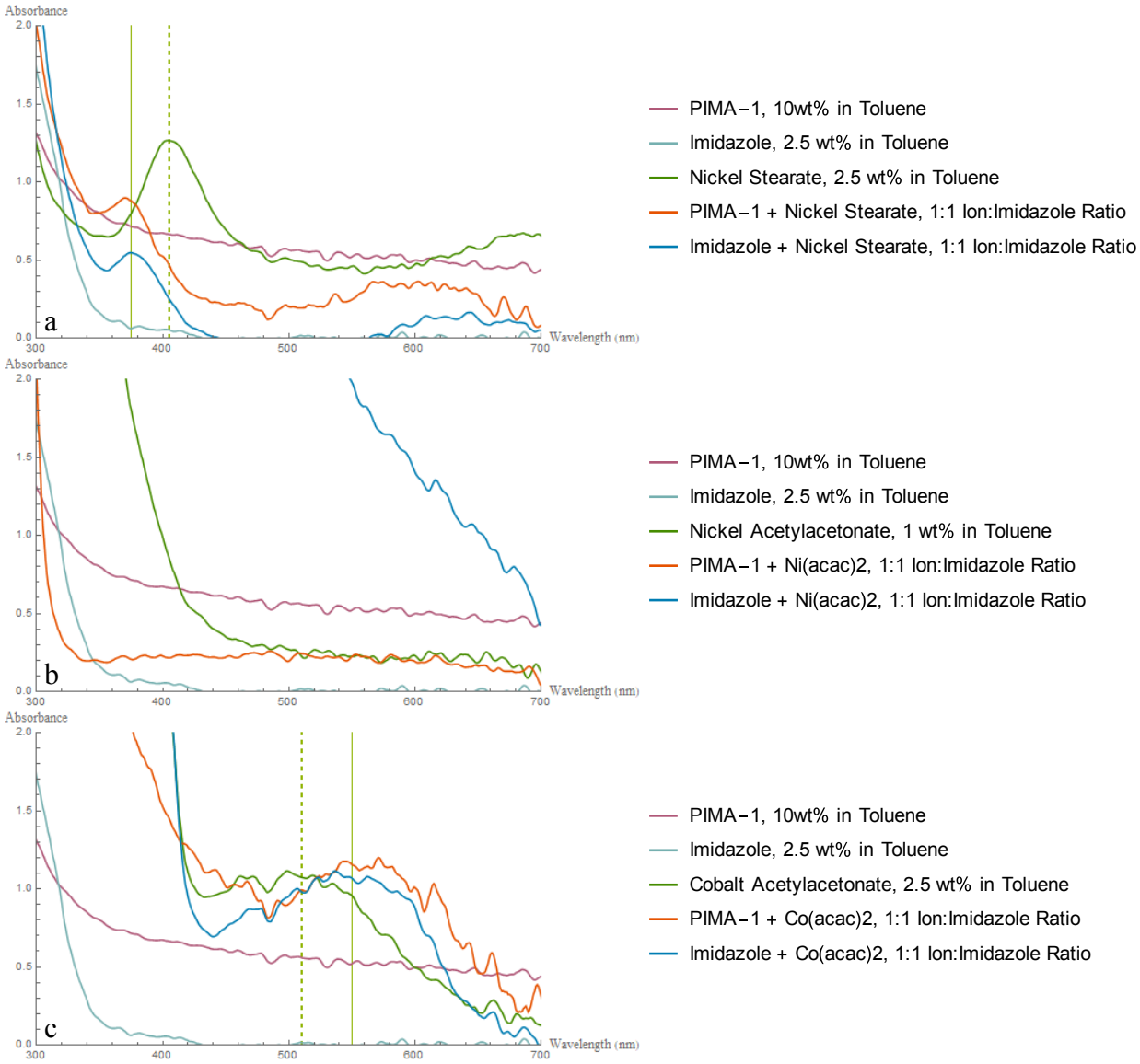

Figure 12: UV-Vis Spectra
a) Nickel Stearate System b) Nickel Acetylacetonate System c) Cobalt Acetylacetonate System

The results of UV-Vis spectroscopy are presented in Figure 12. Figure 12a shows that PIMA-1 and imidazole exhibit a new peak at ~375 nm upon the addition of nickel stearate, suggesting a similar local environment for nickel ions in these solutions. When compared to the peak for the nickel stearate solution at ~405 nm, it is evident that the local nickel environment

has changed, suggesting complexation with imidazoles. A slight difference can be observed between the peak positions for PIMA-1 and imidazole, which may be attributed to weak interactions with other atoms on the histamine moiety.

Results from the nickel acetylacetonate system presented in Figure 12b, are inconclusive with regards to complexation. No distinct peaks can be observed, and the absorbance values appear to be incomparable between samples. Nickel acetylacetonate dissolved poorly in toluene, which may have contributed to the lack of discernible signals. Figure 12c shows the cobalt acetylacetonate system in which PIMA-1 and imidazole both show the emergence of a broad new peak upon the addition of cobalt acetylacetonate at ~500 nm, suggesting cobalt complexation in both systems.

5.2 Rheology results

5.2.1 PIMA Mechanical Properties

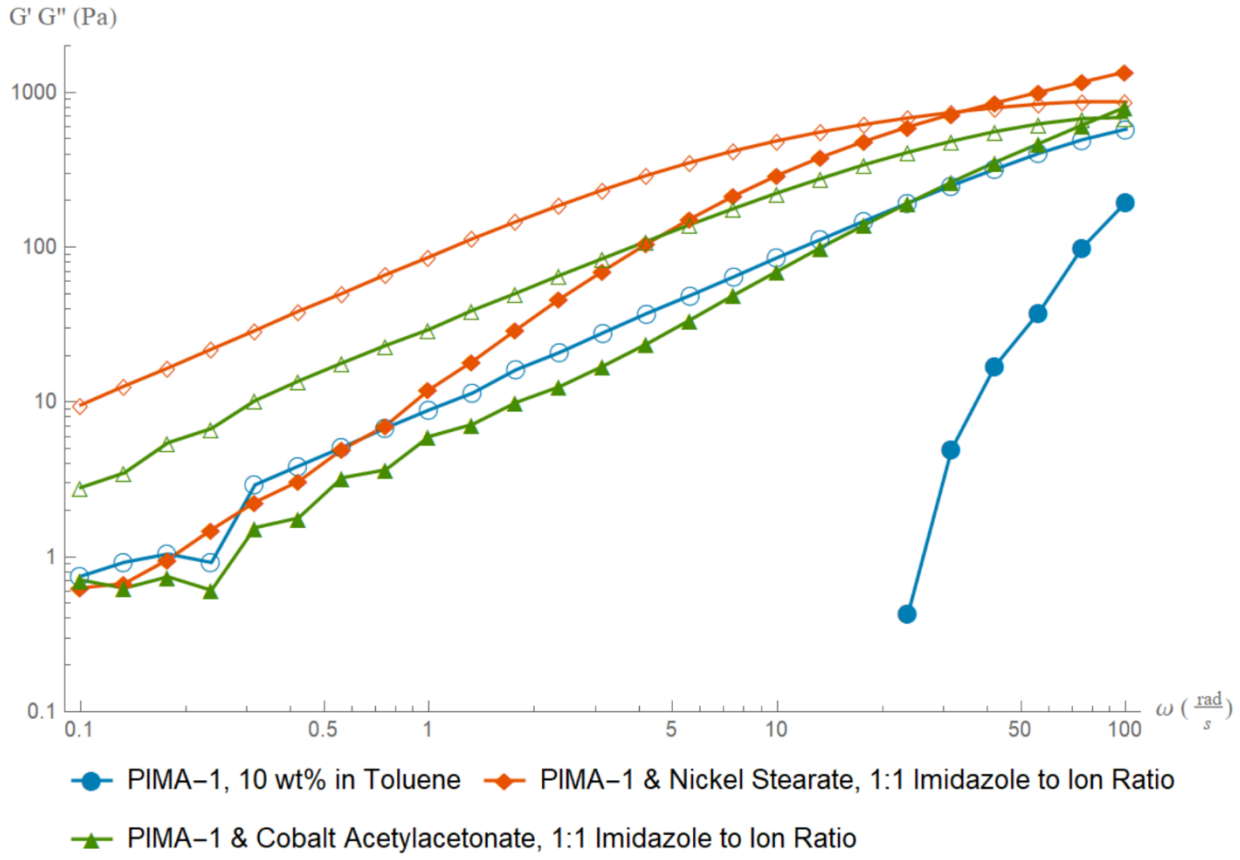

Figure 13: Storage and Loss Moduli of the PIMA-1 system. Closed markers indicate G', open markers indicate G"

The storage (G') and loss (G") moduli of various PIMA-1 solutions are presented in Figure 13. The addition of metal ions increases the storage modulus regardless of ion identity, likely due to metal-coordination crosslinking. The nickel-complexed gel had a higher storage modulus than the cobalt-complexed gel, which is consistent with a higher bond energy for the nickel complexes. The relaxation time, as determined by the inverse of the crossover point of the nickel-complexed gel was also the highest.

5.2.2 PSMA Mechanical Properties

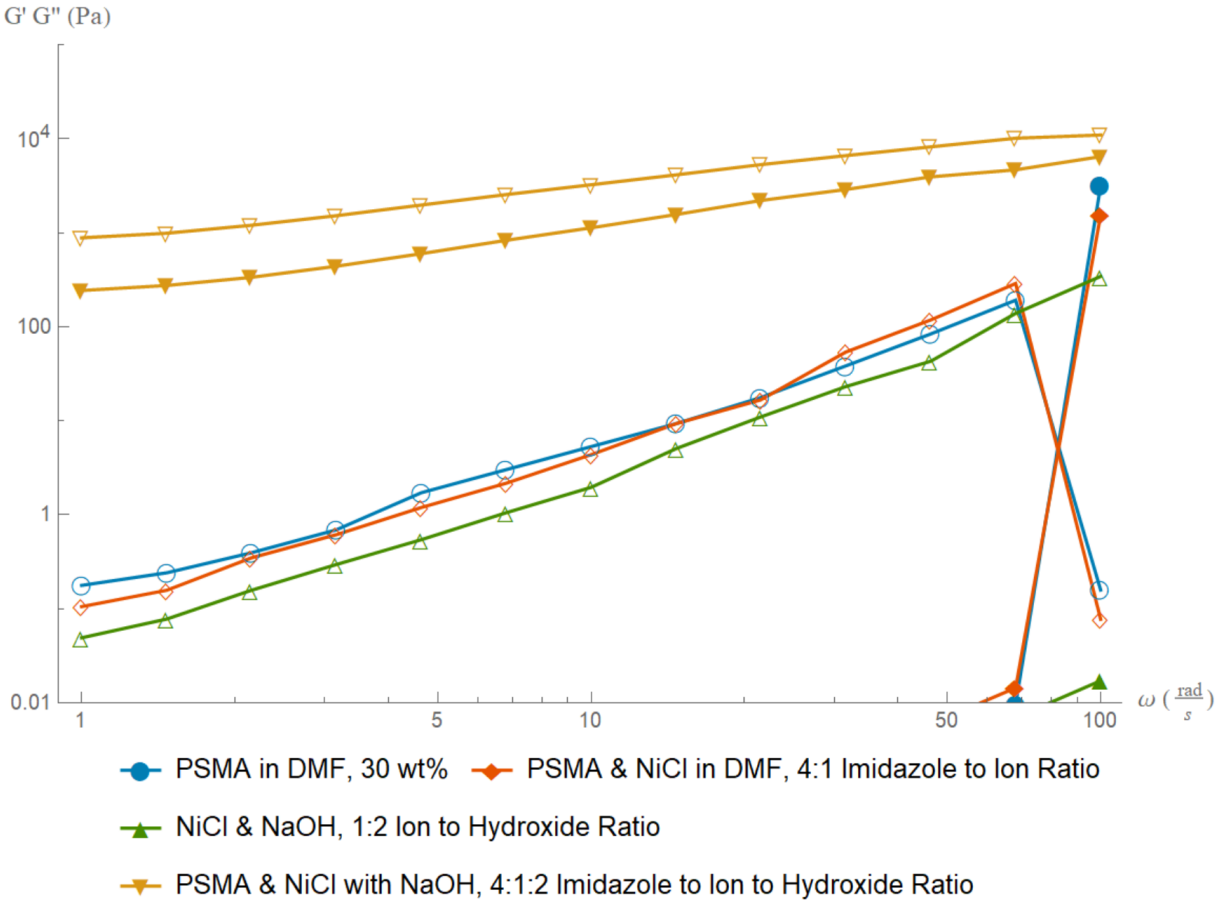

Figure 14: Storage and Loss Moduli of the PSMA-2 system. Closed markers indicate G', open markers indicate G".

The storage (G') and loss (G") moduli of various PSMA solutions are presented in Figure 14. Data with moduli below 0.01 was omitted as noise, and data below 1 rad s^{-1} was omitted due to evaporation effects. The polymer solutions, both with and without metal ions, as well as the nanoparticle suspension, all showed liquid-like character and no measurable storage modulus. The PSMA in this experiment was low molecular weight (M_n~1900), well below the length at which polystyrene begins to exhibit significant viscous effects from entanglement, which may be responsible for its negligible storage modulus. The addition of nickel chloride did not have a significant effect on the PSMA solution, which could possibly be attributed to the stoichiometric ratio in which nickel atoms were added relative to the histamine moieties in the sample. At a 4:1

ratio, the moieties may not be fully saturated due to non-interacting nickel ions shielded by the polar solvent via solvation shells. The nanoparticle suspension was unlikely to form a percolated network of interacting particles due to its diluteness, and the rheological measurements of this sample are likely dominated by the properties of the solvent.

In contrast to the other solutions, the PMSA-NP composite exhibited a measurable storage modulus. This sample precipitated a gelatinous solid surrounded by liquid immediately after NaOH was added. In testing, only the solid was added to the sample stage. The cause of gelation in this system and not the PSMA-Nickel Chloride system is unknown but likely related to the *in-situ* growth of the nanoparticles. $Ni(OH)_2$ particles are uncharged and unlikely to be affected by solvation shells, making nickel-moiety interactions become more likely at the nanoparticle surface.

6. Conclusion & Future Work

In this study, systems of polyisoprene and polystyrene gels in non-aqueous solution were synthesized and characterized. UV-Vis spectroscopy verified the presence of metal coordination of Ni^{2+} and Co^{2+} with histamine moieties grafted onto polyisoprene molecules, all in toluene. Rheological testing showed an increase in storage and loss moduli of polyisoprene gels which was dependent on the ion identity, with Ni^{2+} showing a higher increase. The difference in increases was consistent with the expectation that higher bonding energies between ions and moieties would correlate with higher moduli since the reported bonding energies of Ni^{2+} and Co^{2+} with NH_3 indicate that Ni^{2+} has a higher bonding energy. Rheological testing also showed an increase in relaxation time which was higher for Ni^{2+}, which matches expectations based on bonding energies, as higher bonding energies imply higher activation energy barriers to dissociation. Subsequent work is necessary to verify the correlations with bonding energies by testing different metal ions. Additionally, future experiments will be necessary to establish the effect of crosslink density on mechanical properties in these samples, to evaluate the relative importance of these crosslinks when compared to other molecule interactions such as polymer entanglement.

In-situ nanoparticle growth was achieved in polystyrene gel in DMF, with rheological measurements showing a transition from liquid-like character to viscous character post nanoparticle growth. The mechanisms of the gel formation are not well understood, but are theorized to be the result of the interruption of solvation shells due to nickel ions forming uncharged precipitates of $Ni(OH)_2$ following the addition of sodium hydroxide, thereby enabling moiety-nickel interactions at the particle surface. More testing in the way of microscopy would help to verify the formation of nanoparticles in the gel. Additional testing with variations in

hydrogen ion concentration to suppress $Ni(OH)_2$ precipitation would also help to verify this hypothesis. Lastly, repetition of the experiments in a less volatile solvent would aid in rheological testing, which was impacted by sample evaporation.

By testing various strategies towards the production of mechanically robust polymers crosslinked by metal coordination bonding, we have found that it is possible to form materials with improved mechanical properties when compared to their base polymers through the use of metal coordination chemistry in non-aqueous environments, and that those properties may be controlled by ion identities. We have also demonstrated the novel synthesis of a bottom-up *in-situ* nanocomposite material in a non-aqueous solvent.

7. References

(1) Coran, A. Y. Chapter 7 - Vulcanization. In *The Science and Technology of Rubber (Fourth Edition)*; Mark, J. E., Erman, B., Roland, C. M., Eds.; Academic Press: Boston, 2013; pp 337–381. https://doi.org/10.1016/B978-0-12-394584-6.00007-8.

(2) Grindy, S. C.; Learsch, R.; Mozhdehi, D.; Cheng, J.; Barrett, D. G.; Guan, Z.; Messersmith, P. B.; Holten-Andersen, N. Control of Hierarchical Polymer Mechanics with Bioinspired Metal-Coordination Dynamics. *Nat. Mater.* **2015**, *14* (12), 1210–1216. https://doi.org/10.1038/nmat4401.

(3) Zhang, J.; Hu, Y.; Li, Y. Metal–Organic Gels. In *Gel Chemistry: Interactions, Structures and Properties*; Zhang, J., Hu, Y., Li, Y., Eds.; Lecture Notes in Chemistry; Springer: Singapore, 2018; pp 61–118. https://doi.org/10.1007/978-981-10-6881-2_3.

(4) Li, Q.; Barrett, D. G.; Messersmith, P. B.; Holten-Andersen, N. Controlling Hydrogel Mechanics via Bio-Inspired Polymer–Nanoparticle Bond Dynamics. *ACS Nano* **2016**, *10* (1), 1317–1324. https://doi.org/10.1021/acsnano.5b06692.

(5) Rodgers, M. T.; Armentrout, P. B. Noncovalent Metal–Ligand Bond Energies as Studied by Threshold Collision-Induced Dissociation. *Mass Spectrom. Rev.* **2000**, *19* (4), 215–247. https://doi.org/10.1002/1098-2787(200007)19:4<215::AID-MAS2>3.0.CO;2-X.

(6) OpenStax. 7.5 Strengths of Ionic and Covalent Bonds. In *Chemistry*; 2016.

(7) Mou, C.; Ali, F.; Malaviya, A.; Bettinger, C. J. Electrochemical-Mediated Gelation of Catechol-Bearing Hydrogels Based on Multimodal Crosslinking. *J. Mater. Chem. B* **2019**, *7* (10), 1690–1696. https://doi.org/10.1039/C8TB02854K.

(8) Holten-Andersen, N.; Harrington, M. J.; Birkedal, H.; Lee, B. P.; Messersmith, P. B.; Lee, K. Y. C.; Waite, J. H. PH-Induced Metal-Ligand Cross-Links Inspired by Mussel Yield Self-Healing Polymer Networks with near-Covalent Elastic Moduli. *Proc. Natl. Acad. Sci.* **2011**, *108* (7), 2651–2655. https://doi.org/10.1073/pnas.1015862108.

(9) Skinner, H. C. W.; Jahren, A. H. 8.04 - Biomineralization. In *Treatise on Geochemistry*; Holland, H. D., Turekian, K. K., Eds.; Pergamon: Oxford, 2007; pp 1–69. https://doi.org/10.1016/B0-08-043751-6/08128-7.

(10) Jin, Y.; Kundu, B.; Cai, Y.; Kundu, S. C.; Yao, J. Bio-Inspired Mineralization of Hydroxyapatite in 3D Silk Fibroin Hydrogel for Bone Tissue Engineering. *Colloids Surf. B Biointerfaces* **2015**, *134*, 339–345. https://doi.org/10.1016/j.colsurfb.2015.07.015.

(11) Tambutté, S.; Tambutté, E.; Zoccola, D.; Allemand, D. Organic Matrix and Biomineralization of Scleractinian Corals. In *Handbook of Biomineralization*; John Wiley & Sons, Ltd, 2008; pp 243–259. https://doi.org/10.1002/9783527619443.ch14.

(12) Thoniyot, P.; Tan, M. J.; Karim, A. A.; Young, D. J.; Loh, X. J. Nanoparticle–Hydrogel Composites: Concept, Design, and Applications of These Promising, Multi-Functional Materials. *Adv. Sci.* **2015**, *2* (1–2), 1400010. https://doi.org/10.1002/advs.201400010.

(13) Pinna, N.; Garnweitner, G.; Antonietti, M.; Niederberger, M. A General Nonaqueous Route to Binary Metal Oxide Nanocrystals Involving a C−C Bond Cleavage. *J. Am. Chem. Soc.* **2005**, *127* (15), 5608–5612. https://doi.org/10.1021/ja042323r.